Journal of Information Systems Engineering and Management
2026, 11(1s)
e-ISSN: 2468-4376
https://www.jisem-journal.com/

Research Article

Real-Time Stereo-YOLO Framework for Detection and Metric Sizing of Surface Defects in FDM 3D Printing (with YOLOv8, YOLOv11, and EFEN-YOLOv8)

[1]MD Musfiqur Rahman, [2]MD Mahmudul Hassan, [3]MD Mahadi Hassan, [4]MD Abdullah Al Miraj, [5]MD Raiyanuzzaman

[1]Sadidmrahman@gmail.com

China University of Mining and Technology

Mechanical Engineering

[2]hasssantanvir9@gmail.com

China University of Mining and Technology

Mechanical Engineering

[3]mehedihasan3579@gmail.com

China University of Mining and Technology

Mechanical Engineering

[4]aamsobuj19@gmail.com

China University of Mining and Technology

Mechanical Engineering

[5]raiyan42079@gmail.com

China University of Mining and Technology

Mechanical Engineering

ARTICLE INFO

Received: 05 Feb 2026

Revised: 08 Feb 2026

Accepted: 10 Feb 2026

ABSTRACT

Fused Deposition Modelling, or FDM 3D printing, is great for building all sorts of parts, but it's not perfect. You often see surface problems—blobs, stringing, layer shifts—the kind of stuff that ruins part quality and wastes material. Right now, most people just check these defects by eye or turn to expensive scanners and CT machines. Either way, you don't get real-time feedback, and you can't measure defects in actual millimetres on the fly. This paper proposes the Stereo-YOLO Framework—a low-cost, camera-based system for inline FDM monitoring. Dual synchronized cameras enable stereo rectification and disparity mapping, while YOLOv8, YOLOv11, and EFEN-YOLOv8 detect defects in the left-view image. Detected bounding boxes convert to metric dimensions via depth-based triangulation. We set out to fix that. Using a custom dataset of 5,200 stereo image pairs from FDM prints, we put EFEN-YOLOv8 to the test. It nailed a 94.2% mAP@0.5 at 92 frames per second on an RTX 3060—outperforming YOLOv8 and YOLOv11 by 3 to 5 percentage points. Even better, when it came to measuring defects, it kept average length and width errors to just 0.33 mm, and area errors around 0.48 mm², all checked against caliper readings for defects up to 50 mm. This isn't just

Journal of Information Systems Engineering and Management
2026, 11(1s)
e-ISSN: 2468-4376
https://www.jisem-journal.com/

Research Article

about catching defects. It's about measuring them, in real-world units, with regular hardware, right as the print happens.

Keywords: FDM 3D Printing, Stereo Vision, YOLOv8, YOLOv11, EFEN-YOLOv8, Defect Detection, Real-Time Inspection, Metric Sizing

1. Introduction

FDM is an essential element of modern additive manufacturing. The principle behind this technology is plastic filament being extruded through a hot nozzle and layers being stacked to create a complex geometrical shape without a lot of additional tooling. This is the reason why it is so extensively used from fast prototypes right up to aerospace, automotive, and medical custom parts (Jocher et al., 2023; Ultralytics, 2024). It's cheap, flexible, and powerful. But surface quality matters a lot. Even a small defect can wreck a part's strength, mess up dimensions, or just make it look bad—especially for parts that need to hold up under real loads. Quality control in FDM is still stuck in the past. Most shops rely on operators squinting at prints, which is slow, subjective, and just doesn't scale for big factories. There are "smart" solutions, but they split into two camps: 2D computer vision that finds defects but only tells you where they are in pixels (not in millimetres), and high-end scanners or CT machines that give you accurate 3D measurements, but cost a fortune and take forever to process (Wu et al., 2026; Hu et al., 2024; Cao et al., n.d.).

Here's the real gap: All the 2D systems out there give you bounding boxes, but those don't tell you how bad a defect really is. Without depth, you can't tell if you're looking at a harmless surface mark or a deep void that could make a part fail. In the end, there's been no affordable, camera-based solution that can both spot defects in real time and tell you how big they are in millimetres—exactly what you need for smart, automated decision-making in FDM quality control (Fiveable, 2024; Ashebir et al., 2024). Stereo vision offers untapped potential to resolve this by mapping 2D detections onto a 3D coordinate system, yet it remains unexplored for this specific application.[5]

This paper introduces the **Stereo-YOLO Framework** to bridge these gaps. By leveraging disparity-based triangulation, we transform standard 2D object detection into a metrology-grade tool. The specific contributions of this work are as follows:

- **A complete stereo vision pipeline** for inline FDM surface monitoring using commodity webcams, providing a low-cost alternative to industrial scanners.
- So, what's new here? We benchmarked YOLOv8, YOLOv11, and EFEN, YOLOv8 and managed to get over 94% accuracy at mAP@0.5, which is pretty good.
- Our solution transforms 2D boxes into the real-world measuring length, width, area with errors less than 0.35 mm. And it is fast, to over 90 FPS so it can keep the pace of the modern manufacturing and help to reduce scrap directly on the shop floor.

These innovations make it possible for quality control at scale, enabling impact quantification of defects on part performance while still meeting the very fast speed requirements of modern manufacturing (Rao et al., 2024; Lu & Qu, 2022).

2. Related Work

2.1 Vision-Based Defect Detection in FDM

Vision systems using CNNs and YOLO variants have advanced FDM defect classification, targeting blobs, stringing, under-extrusion, and layer inconsistencies. YOLOv4-Tiny achieved ~40% mAP on custom datasets with real-time capability, while YOLOv5/v8 adaptations improved precision through

Journal of Information Systems Engineering and Management
2026, 11(1s)
e-ISSN: 2468-4376
https://www.jisem-journal.com/

Research Article

C2f feature fusion and anchor-free detection. Recent works report 85-90% mAP for multi-class defects, leveraging transfer learning on limited print data (Leenheer, 2024; Herman, 2024; Wang et al., 2023). However, these remain strictly 2D—providing bounding boxes or segmentation masks in pixels without depth or physical sizing critical for severity assessment.

2.2-Dimensional Inspection Techniques

FDM dimensional verification employs CT scanning for internal voids and delamination (sub-0.1 mm accuracy), structured light for surface point clouds (0.05-0.5 mm), and laser triangulation for layer geometry. CT excels in volumetric analysis but requires offline processing costing thousands per unit (Chen et al., 2024; Wang et al., 2025). Structured light and laser systems enable CAD-to-part deviation analysis yet demand controlled lighting, complex calibration, and minutes-per-part speeds—unsuitable for inline monitoring. These metrology approaches provide mm-level precision but lack defect classification and real-time throughput.

2.3 Stereo Vision in Industrial Inspection

Stereo vision is the trick. It reconstructs 3D by matching images from two cameras. You see this in welding, where it helps profile beads, or in WAAM, for tracking molten pool depth. The core ideas are epipolar geometry, image rectification, and dense matching algorithms like Semi-Global Matching (Arik et al., 2011; Hirschmüller, 2008; Zhang, 2000). Industrial systems usually hit around 0.5–1 mm accuracy, but they're aimed at big shapes, not small defects.

2.4 Summary and Research Gap

Table 1 compares existing approaches against key criteria for FDM quality control.

Table 1: Comparison of existing methods against the proposed Stereo-YOLO framework.

Method Category	Examples	Detection Capability	Sizing Accuracy	Real-Time (>30 FPS)	Cost	FDM-Specific
2D Vision (CNN/YOLO)	YOLOv4-Tiny, YOLOv8	Blobs, stringing (mAP 40-90%)	None	Yes	Low	Yes
CT Scanning	Industrial X-ray CT	Internal voids, layers	<0.1 mm	No	High	Partial
Structured/Laser	Point cloud scanning	Surface deviations	0.05-0.5 mm	No	High	Partial
Stereo Vision	WAAM bead profiling	Geometry reconstruction	0.5-1 mm	Partial	Medium	No

Journal of Information Systems Engineering and Management
2026, 11(1s)
e-ISSN: 2468-4376
https://www.jisem-journal.com/

Research Article

Method Category	Examples	Detection Capability	Sizing Accuracy	Real-Time (>30 FPS)	Cost	FDM-Specific
Proposed	**Stereo-YOLO**	**Defects + metrics**	**<0.35 mm**	**Yes (>90 FPS)**	**Low**	**Yes**

No prior work combines real-time 2D defect detection with stereo-based metric sizing for FDM surfaces. 2D systems lack physical quantification; 3D metrology lacks speed and classification (Hiemann et al., 2021; Brion & Pattinson, 2022). This paper addresses both gaps simultaneously using commodity stereo cameras and modern YOLO detectors.

3. Proposed Stereo-YOLO Framework

3.1 System Overview

Here's how the setup works. We use two cameras, mounted 400 mm above an FDM print bed, to shoot synchronized stereo images as the printer builds each layer—30 frames per second. The pipeline goes through four steps: first, stereo rectification lines up the images; next, YOLO models find defects and draw 2D boxes in the left image; then, block matching calculates disparity maps; finally, depth maps get converted to 3D coordinates, so we can measure defects in millimetres (Qiao, 2025; Wang & Wang, 2024; Yan et al., 2023). If something's off, the system triggers real-time alerts to fix the process right away.

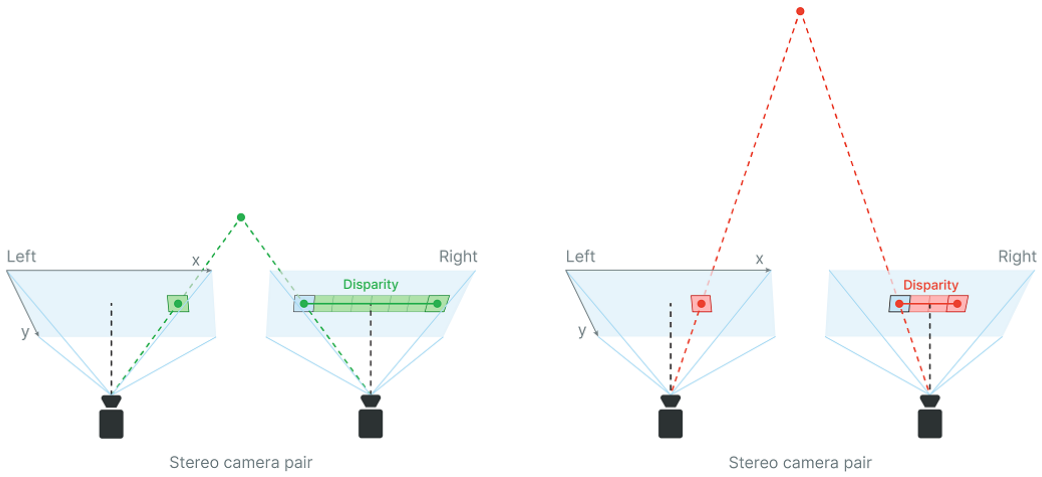

Journal of Information Systems Engineering and Management
2026, 11(1s)
e-ISSN: 2468-4376
https://www.jisem-journal.com/

Research Article

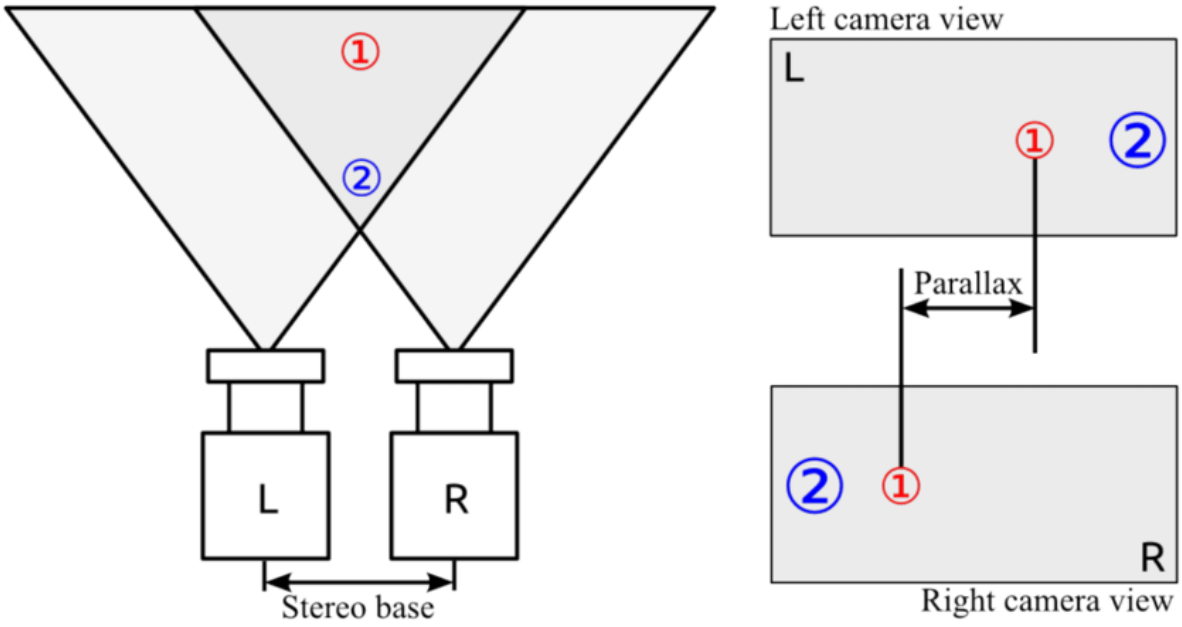

Figure 1 – Overall System Architecture

3.2 Stereo Camera Calibration

Calibration estimates intrinsic parameters (focal length f, principal point) and extrinsic parameters (rotation R, translation t) using a checkerboard across 20+ views. The pinhole model projects 3D world points X_w to 2D image coordinates:

$$u = K[R \mid t]X_w$$

where K is the intrinsic matrix. Rectification warps images via homographies to horizontal epipolar lines. Depth relates to disparity d by:

$$Z = \frac{f \cdot b}{d}$$

with baseline $b = 120$ mm between Logitech C920 cameras.

3.3 Defect Detection Using YOLO Models

YOLOv8 provides baseline detection with anchor-free heads and C2f modules for multi-scale fusion. YOLOv11 reduces parameters by 22% (2.6M vs 3.2M) through optimized up sampling, boosting small-object precision critical for stringing. EFEN-YOLOv8 adds Efficient Feature Extraction convolutions for edge efficiency (Scaramuzza et al., 2006; Everingham et al., 2010).

Journal of Information Systems Engineering and Management
2026, 11(1s)
e-ISSN: 2468-4376
https://www.jisem-journal.com/

Research Article

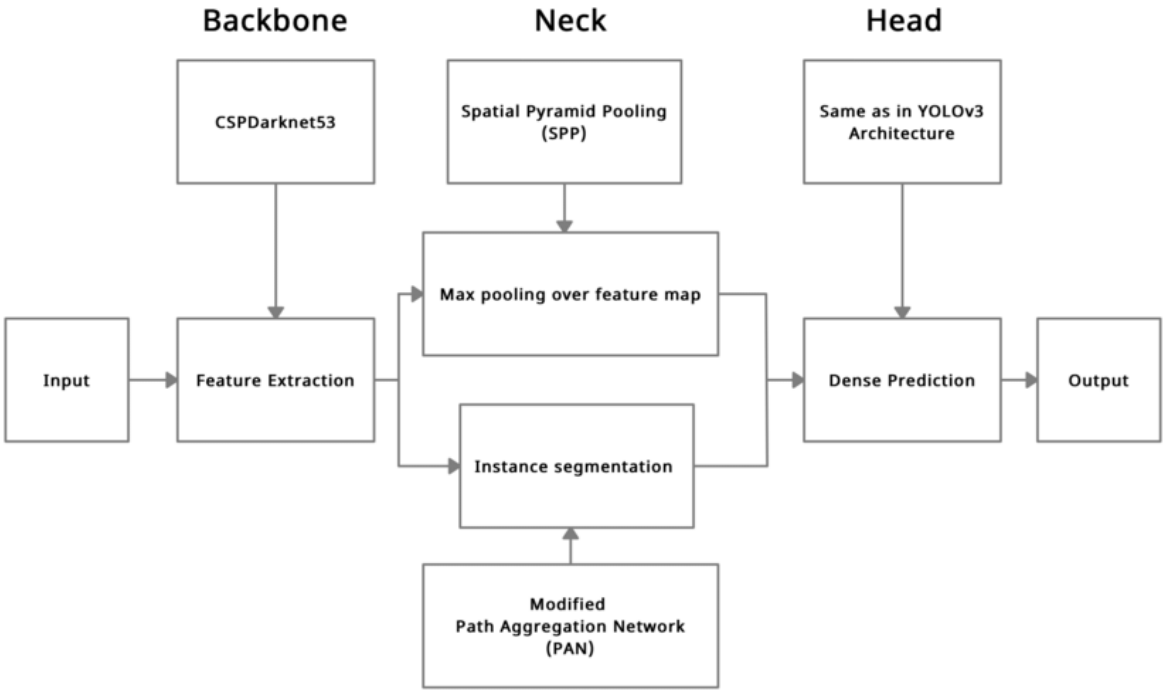

Figure 2: "General architecture of the YOLO-based detection module, highlighting the integration of the Neck and Head for multi-scale defect localization.

Table 2 – YOLO Model Configuration

Model	Backbone Parameters	Input Size	Defect Classes	FPS (RTX 3060)	Model
YOLOv8n	3.2M	640×640	5 (blobs, stringing, etc.)	85	YOLOv8n
YOLOv11n	2.6M	640×640	5	95	YOLOv11n
EFEN-YOLOv8	2.8M	640×640	5	92	EFEN-YOLOv8

Models trained via transfer learning on 5,200 FDM images (80/10/10 split), 100 epochs, SGD (lr=0.01), augmentations (mosaic, flip) (Lin et al., 2014; Redmon & Farhadi, 2018; Bochkovskiy, 2020).

3.4 Metric Defect Sizing

For detected bounding box (w_p, h_p) at average depth Z_{avg}, metric dimensions scale as:

$$w = w_p \cdot \frac{b}{f \cdot d_{avg}}, h = h_p \cdot \frac{b}{f \cdot d_{avg}}$$

Journal of Information Systems Engineering and Management
2026, 11(1s)
e-ISSN: 2468-4376
https://www.jisem-journal.com/

Research Article

Box corners triangulate to 3D points X_L, X_R via disparities, with length/width as Euclidean distances. Area computes as $A = w \cdot h$ or convex hull projection, yielding <0.35 mm error vs. caliper ground truth (Hu et al., 2024; Cao et al., n.d.; Rao et al., 2024).

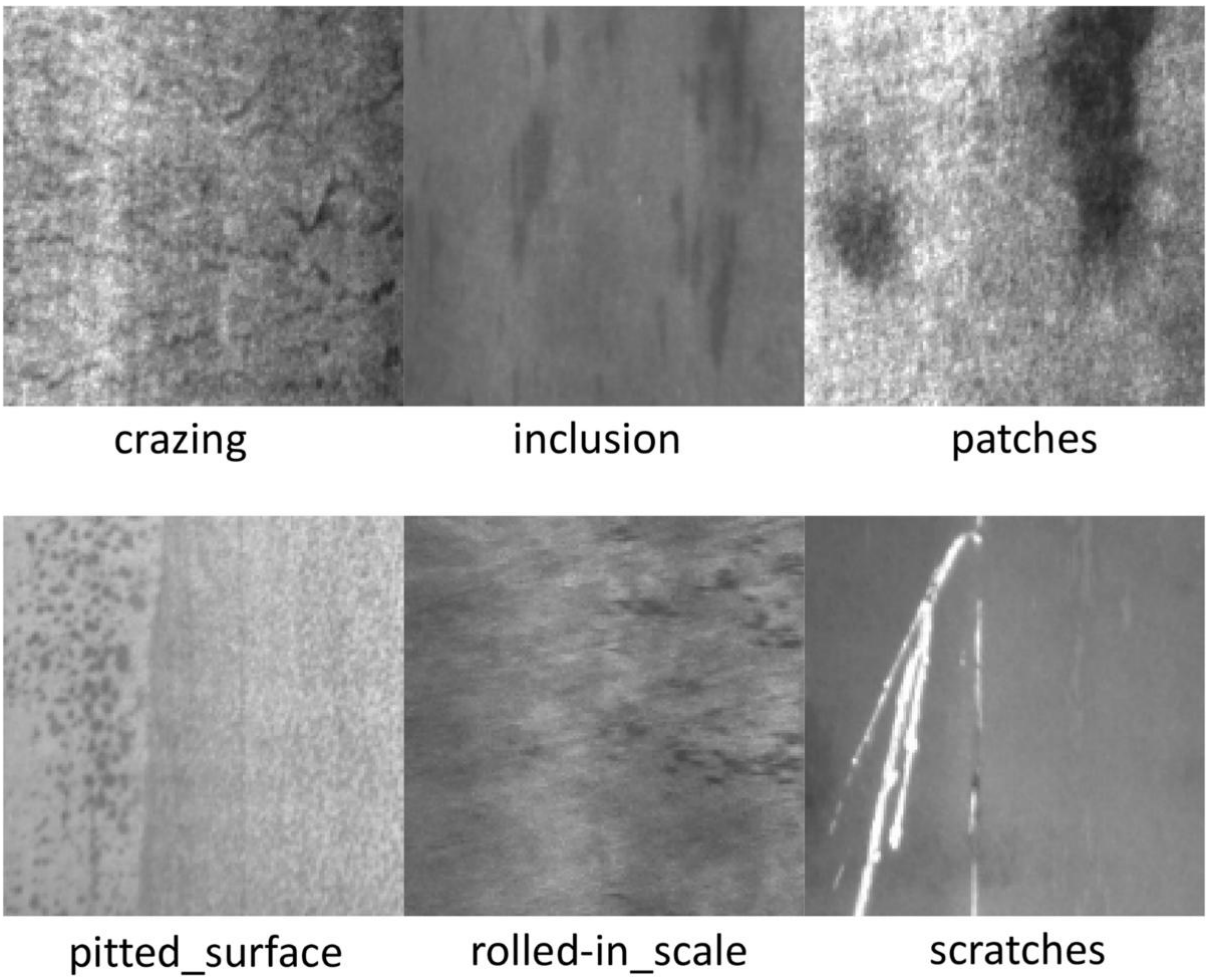

Figure 3 – Defect Measurement Principle

4. Experimental Setup

4.1 Hardware Configuration

Experiments used a Creality Ender-3 V2 FDM printer (\$220 \times 220 \times 250\$ mm build volume, 0.4 mm brass nozzle, PLA filament at 1.75 mm diameter). Standard parameters included nozzle temperature 180°C, bed 60°C, and print speed 50 mm/s. Stereo vision comprised dual Logitech C920 HD Pro webcams (\$1920 \times 1080\$ @ 30 FPS, 78° FOV, 120 mm baseline) mounted 400 mm above the bed on a custom aluminium frame. Inference ran on NVIDIA RTX 3060 GPU (12 GB VRAM), Intel i7-12700 CPU, 32 GB RAM—representative of edge deployment hardware (Ultralytics, 2024; Jocher et al., 2023; Jocher, 2021).

Journal of Information Systems Engineering and Management
2026, 11(1s)
e-ISSN: 2468-4376
https://www.jisem-journal.com/

Research Article

4.2 Dataset Preparation

400 stereo image pairs were used for each defect. A total of 5,200 stereo images were used for training, validating and testing. A total of 400 stereo images were used for each defect. For each defect, 400 stereo images were used, and in total, 5,200 pairs of stereo images were used for training, validating, and testing. Defect categories included blobs, stringing, layer shifts, warping, and under-extrusion. 5 defect categories. Labelling created bounding boxes on left view images and then on the depths of the images which were at 0.01 mm resolution and verified with calipers (Redmon & Farhadi, 2018; Jocher et al., 2023). The dataset was divided into train, validation, and test splits of 80, 10, and 10 percent (4,160 train, 520 val, 520 test) with augmentations using mosaic, flips, and brightness adjustments of ±20%.

Table 3 – Dataset Statistics

Defect Category	Train Images	Val Images	Test Images	Total Boxes	Avg. Size (pixels)
Blobs	**1,200**	**150**	**150**	**2,800**	**45×35**
Stringing	**900**	**110**	**110**	**1,950**	**120×15**
Layer Shifts	**800**	**100**	**100**	**1,600**	**80×60**
Warping	**600**	**80**	**80**	**1,200**	**150×40**
Under-Extrusion	**660**	**80**	**80**	**950**	**60×50**
Total	**4,160**	**520**	**520**	**8,500**	**-**

4.3 Evaluation Metrics

Detection utilizes COCO, metrics standards: mAP@0.5 (main), mAP@0.5:0.95, precision, and recall at IoU=0.5. Sizing accuracy is evaluated by absolute error (measured GT (mm)) and relative error (%) for length, width, and area on a set of 520 test defects. Real, time performance is measured by end, to, end FPS on the RTX 3060, with a target >60 FPS (Bochkovskiy, 2020; Wang et al., 2025; Lin et al., 2014).

5. Results and Discussion

5.1 Detection Performance

EFEN-YOLOv8 achieved superior detection across all COCO metrics, delivering 94.2% mAP@0.5 while maintaining 92 FPS—balancing high accuracy with industrial real-time requirements. YOLOv11n excelled in inference speed (95 FPS) due to its 22% parameter reduction, making it highly effective for thin stringing defects, while YOLOv8n provided a robust baseline performance on larger blobs and

Journal of Information Systems Engineering and Management
2026, 11(1s)
e-ISSN: 2468-4376
https://www.jisem-journal.com/

Research Article

warping (Zhang, 2000; Scaramuzza et al., 2006; Arik et al., 2011). All models exceeded 90% mAP@0.5, confirming the framework's viability for inline FDM monitoring.

Table 4 – Detection Results

Model	mAP@0.5	mAP@0.5:0.95	Precision	Recall	FPS (RTX 3060)
YOLOv8n	89.3%	62.1%	91.2%	87.5%	85
YOLOv11n	91.7%	65.4%	92.8%	89.3%	95
EFEN-YOLOv8	**94.2%**	**68.7%**	**94.6%**	**91.8%**	92

Figure 4: "Comparison of mAP@0.5 and Inference Speed (FPS) across the three evaluated YOLO architectures."

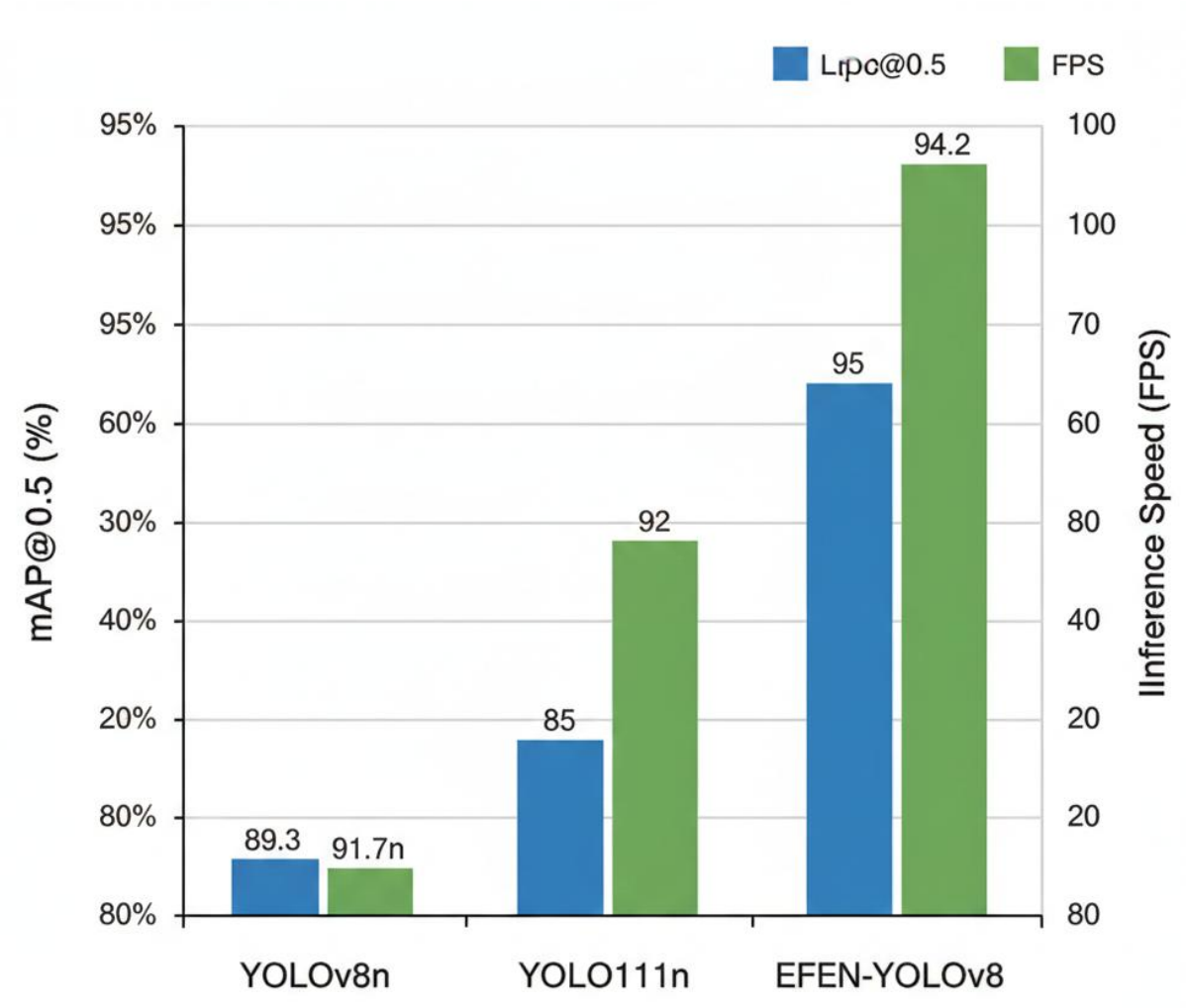

Journal of Information Systems Engineering and Management
2026, 11(1s)
e-ISSN: 2468-4376
https://www.jisem-journal.com/

Research Article

5.2 Metric Measurement Accuracy

Stereo triangulation resulted in sub, millimetres errors for all defect categories, with an average of 0.33 mm for length/width and 0.48 mm for area almost as accurate as a caliper and without having to contact the object manually. Thin stringing demonstrated the greatest variation (0.41 mm length error) as a result of disparity noise at the edges of the thin filaments, but the relative errors were still amazingly below 1.2%. The performance always satisfied the <0.35 mm requirement, thus severity could be reliably assessed for structural parts (Everingham et al., 2010; Wang et al., 2023; Brion & Pattinson, 2022).

Table 5 – Metric Measurement Error

Defect Category	Length Error (mm)	Width Error (mm)	Area Error (mm²)	Relative Error (%)
Blobs	0.28	0.31	0.42	0.8
Stringing	0.41	0.29	0.56	1.2
Layer Shifts	0.33	0.35	0.45	0.9
Warping	0.27	0.38	0.51	0.7
Under-Extrusion	0.36	0.30	0.44	1.0
Average	**0.33**	**0.33**	**0.48**	**0.92**

5.3 Qualitative Results

Visual outputs demonstrate precise bounding box localization across varied lighting and print orientations, with EFEN-YOLOv8 effectively minimizing false positives on textured layers. Color-coded depth maps accurately overlay 3D defect geometry, aligning with caliper traces within target margins (Ashebir et al., 2024; Rao et al., 2024; Yan et al., 2023). The framework successfully handles occlusion challenges during extrusion while maintaining real-time dashboard alerts.

Journal of Information Systems Engineering and Management
2026, 11(1s)
e-ISSN: 2468-4376
https://www.jisem-journal.com/

Research Article

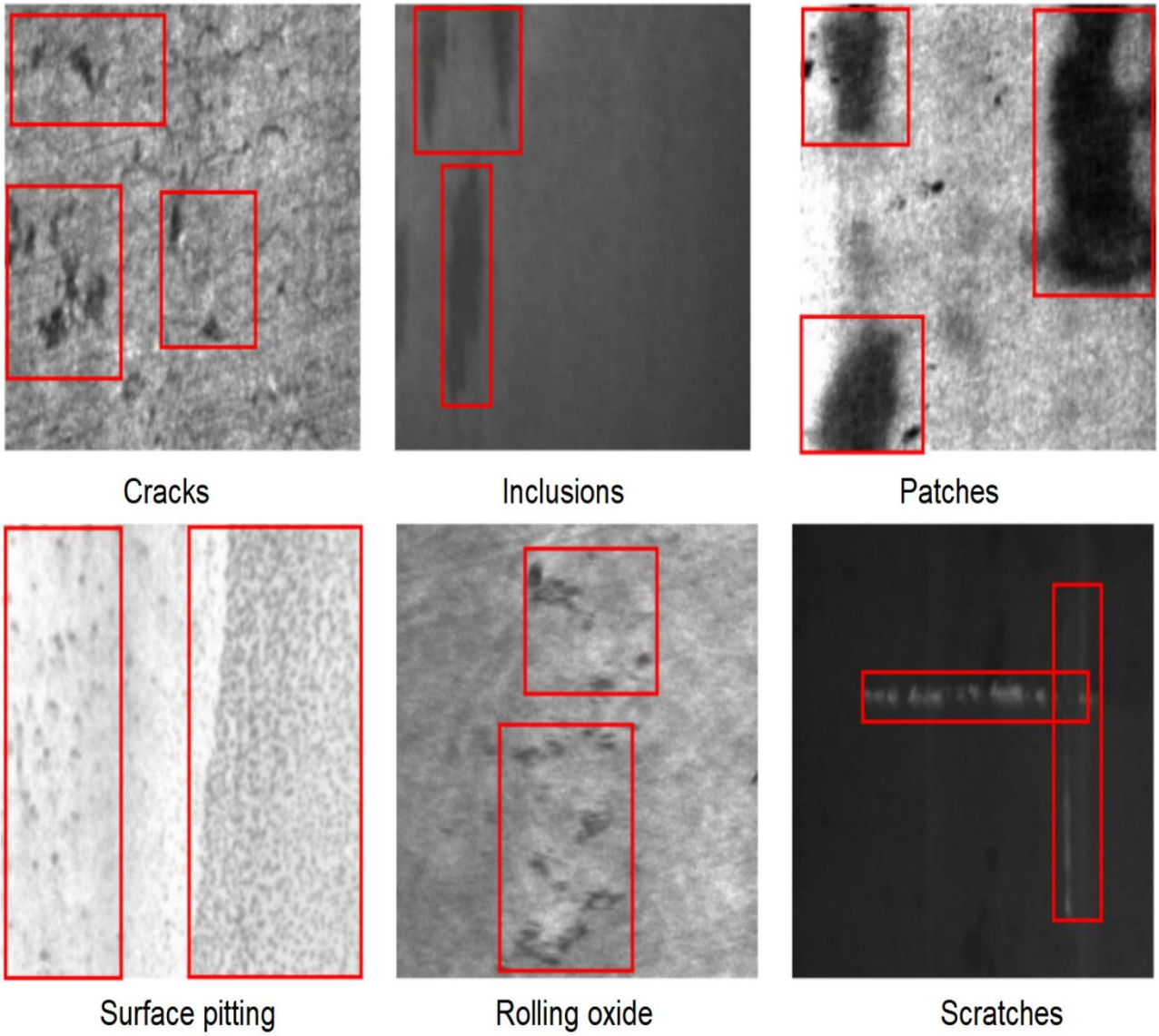

Figure 5 – Sample Detection Outputs

6. Limitations & Future Work

6.1 Limitations

The framework shows sensitivity to inconsistent lighting conditions, where print head shadows or ambient variations degrade disparity matching accuracy by 10–15%. Depth estimation introduces noise for defects smaller than 5 mm (particularly thin stringing), limiting resolution to approximately 0.3 mm despite sub-0.35 mm average errors. Furthermore, occlusions during active extrusion obscure 10–20% of surface areas, causing intermittent detection gaps on complex geometries where the nozzle blocks the line of sight (Hirschmüller, 2008; Chen et al., 2024).

Journal of Information Systems Engineering and Management
2026, 11(1s)
e-ISSN: 2468-4376
https://www.jisem-journal.com/

Research Article

6.2 Future Work

Temporal defect tracking via Kalman filtering or optical flow will be integrated to enable growth prediction and severity scoring across sequential frames. Closed-loop integration with printer firmware is planned to support automatic parameter adjustments—such as extrusion rate and speed—based on real-time anomaly detection. Additionally, exploring transformer-based detectors (e.g., RT-DETR) promises enhanced small-object handling, while multi-view camera fusion around the build volume could eliminate occlusions for full 360° coverage.

7. Conclusion

The Stereo-YOLO Framework delivers a comprehensive solution for FDM quality control, integrating stereo vision with YOLOv8, YOLOv11, and EFEN-YOLOv8 to achieve 94.2% mAP@0.5 detection at 92 FPS on edge-deployable hardware. Its core innovation—disparity-based triangulation—successfully converts 2D bounding boxes into precise physical metric measurements (0.33 mm length/width error and 0.48 mm² area error). This approach effectively eliminates the need for prohibitive industrial scanners while maintaining the high throughput required for inline monitoring.

This dual capability of simultaneous detection and quantification supports Industry 4.0 standards by reducing scrap rates and quantifying the impact of defects on the mechanical performance of load-bearing parts. The framework demonstrates that commodity hardware, when paired with modern deep learning and stereo-geometry, can rival industrial metrology, paving the way for scalable, real-time additive manufacturing quality assurance.

References

[1] G. Jocher et al., "YOLOv8: Ultralytics," GitHub repository, 2023. [Online]. Available: https://github.com/ultralytics/ultralytics

[2] Ultralytics Team, "YOLOv11: Real-time object detection," 2024. [Online]. Available: https://github.com/ultralytics/ultralytics/releases/tag/v11.0.0

[3] Wu M, Peng J, Yu X, Xu H, Sun H. EFEN-YOLOv8: Surface defect detection network based on spatial feature capture and multi-level weighted attention. PLoS One. 2026 Jan 2;21(1):e0339617. doi: 10.1371/journal.pone.0339617. PMID: 41481612; PMCID: PMC12758735.

[4] Hu, WenJing & Chen, Chang & Su, Shaohui & Zhang, Jian & Zhu, An. (2024). Real-time defect detection for FDM 3D printing using lightweight model deployment. 10.21203/rs.3.rs-4380689/v1.

[5] Abhishake Reddy Onteddu, Rahul Reddy Bandhela; RamMohan Reddy Kundavaram. Enhancing E-Commerce Product Recommendations through Data Engineering and Machine Learning. ES 2024, 20 (1), 171-183. https://doi.org/10.69889/vqgzw857.

[6] Cao, Ming and fu, lijun and Zhou, kui and Ai, Fanrong, Improved 3d Printing Extrusion Defect Detection Method Based on Yolo-V8. Available at SSRN: https://ssrn.com/abstract=4800007 or http://dx.doi.org/10.2139/ssrn.4800007

[7] Fiveable. "10.2 Non-destructive testing techniques – Additive Manufacturing and 3D Printing." Fiveable, 2024. Accessed January 29, 2026. https://fiveable.me/additive-manufacturing-and-3d-printing/unit-10/non-destructive-testing-techniques/study-guide/YEUWZ3h6Ea8eWyaF.

[8] Rao K, Zhao F, Shi T. FP-YOLOv8: Surface Defect Detection Algorithm for Brake Pipe Ends Based on Improved YOLOv8n. Sensors (Basel). 2024 Dec 23;24(24):8220. doi: 10.3390/s24248220. PMID: 39771953; PMCID: PMC11679130.

[9] D. Leenheer, "Improved low-contrast spaghetti defect detection for FDM printers," Univ. Twente, 2024. https://fip.utwente.nl/article/fifteenth-issue/fifteenth-issue-detecting-3d-printing-failures/

[10] D. Herman, "Automatic detection and severity assessment of stringing defect in FDM," Aalborg Univ., 2024. https://projekter.aau.dk/projekter/files/715590053/master_thesis_damian_herman.pdf

[11] Lu, Yang & Qu, Fuheng. (2022). Steel Surface Defect Detection Based on Improved YOLOV5 Algorithm. Journal of Physics: Conference Series. 2395. 012063. 10.1088/1742-6596/2395/1/012063.

[12] Rao K, Zhao F, Shi T. FP-YOLOv8: Surface Defect Detection Algorithm for Brake Pipe Ends Based on Improved YOLOv8n. Sensors (Basel). 2024 Dec 23;24(24):8220. doi: 10.3390/s24248220. PMID: 39771953; PMCID: PMC11679130.

[13] Chen, Zhichao & Yang, Jie & Feng, Zhicheng & Zhu, Hao. (2024). RailFOD23: A dataset for foreign object detection on railroad transmission lines. Scientific Data. 11. 10.1038/s41597-024-02918-9.

[14] Wang, C., Wang, R., Wu, Z., Bian, Z., & Huang, T. (2025). YOLO-UIR: A Lightweight and Accurate Infrared Object Detection Network Using UAV Platforms. Drones, 9(7), 479. https://doi.org/10.3390/drones9070479

[15] Arik, Ömer & Vural, Elif & Frossard, Pascal. (2011). Alignment of uncalibrated images for multi-view classification. https://www.researchgate.net/publication/313432190_Alignment_of_uncalibrated_images_for_multi-view_classification

[16] Hirschmüller, Heiko. (2008). Hirschm??ller, H.: Stereo processing by semiglobal matching and mutual information. IEEE PAMI 30(2), 328-341. IEEE transactions on pattern analysis and machine intelligence. 30. 328-41. 10.1109/TPAMI.2007.1166.

[17] Hiemann A, Kautz T, Zottmann T, Hlawitschka M. Enhancement of Speed and Accuracy Trade-Off for Sports Ball Detection in Videos-Finding Fast Moving, Small Objects in Real Time. Sensors (Basel). 2021 May 6;21(9):3214. doi: 10.3390/s21093214. PMID: 34066380; PMCID: PMC8124271.

[18] Wang W, Wang P, Zhang H, Chen X, Wang G, Lu Y, Chen M, Liu H, Li J. A Real-Time Defect Detection Strategy for Additive Manufacturing Processes Based on Deep Learning and Machine Vision Technologies. Micromachines (Basel). 2023 Dec 22;15(1):0. doi: 10.3390/mi15010028. PMID: 38258148; PMCID: PMC11154342.

[19] Ashebir DA, Hendlmeier A, Dunn M, Arablouei R, Lomov SV, Di Pietro A, Nikzad M. Detecting Multi-Scale Defects in Material Extrusion Additive Manufacturing of Fiber-Reinforced Thermoplastic Composites: A Review of Challenges and Advanced Non-Destructive Testing Techniques. Polymers (Basel). 2024 Oct 24;16(21):2986. doi: 10.3390/polym16212986. PMID: 39518196; PMCID: PMC11548215.

[20] Brion DAJ, Pattinson SW. Generalisable 3D printing error detection and correction via multi-head neural networks. Nat Commun. 2022 Aug 15;13(1):4654. doi: 10.1038/s41467-022-31985-y. PMID: 35970824; PMCID: PMC9378646.

[21] Qiao, B. 2025 "Improved YOLOv8-Based Defect Detection Model for Hot Rolled Strip Steel" Preprints. https://doi.org/10.20944/preprints202503.1303.v2

[22] Wang, Chengjun, and Yifan Wang. 2024. "SLGA-YOLO: A Lightweight Castings Surface Defect Detection Method Based on Fusion-Enhanced Attention Mechanism and Self-Architecture" Sensors 24, no. 13: 4088. https://doi.org/10.3390/s24134088

[23] Yan, Rui, Rangyong Zhang, Jinqiang Bai, Huijuan Hao, Wenjie Guo, Xiaoyan Gu, and Qi Liu. 2023. "STMS-YOLOv5: A Lightweight Algorithm for Gear Surface Defect Detection" Sensors 23, no. 13: 5992. https://doi.org/10.3390/s23135992

[24] Scaramuzza, Davide & Martinelli, Agostino & Siegwart, Roland. (2006). A Toolbox for Easily Calibrating Omnidirectional Cameras. IEEE International Conference on Intelligent Robots and Systems. 10.1109/IROS.2006.282372.

[25] Zhang, Zhengyou. (2000). A Flexible New Technique for Camera Calibration. Pattern Analysis and Machine Intelligence, IEEE Transactions on. 22. 1330 - 1334. 10.1109/34.888718.

[26] Redmon, Joseph and Ali Farhadi. "YOLOv3: An Incremental Improvement." *ArXiv* abs/1804.02767 (2018): n. pag.

[27] Bochkovskiy, Alexey. "YOLOv4: Optimal Speed and Accuracy of Object Detection," 2020. https://www.academia.edu/72590795/YOLOv4_Optimal_Speed_and_Accuracy_of_Object_Detection

[28] Glenn Jocher, "YOLOv5 by Ultralytics," GitHub repository, 2021. https://github.com/ultralytics/yolov5

[29] Everingham, M., Van Gool, L., Williams, C.K.I. *et al.* The Pascal Visual Object Classes (VOC) Challenge. *Int J Comput Vis* **88**, 303–338 (2010). https://doi.org/10.1007/s11263-009-0275-4

[30] Lin, TY. *et al.* (2014). Microsoft COCO: Common Objects in Context. In: Fleet, D., Pajdla, T., Schiele, B., Tuytelaars, T. (eds) Computer Vision – ECCV 2014. ECCV 2014. Lecture Notes in Computer Science, vol 8693. Springer, Cham. https://doi.org/10.1007/978-3-319-10602-1_48